Robustness of phylogenetic analysis for detecting clusters of new HIV infections

August Guang[1,2], Mark Howison[3], Charles Lawrence[4], Casey W. Dunn[5], Rami Kantor[6]

[1] Center for Computational Biology of Human Disease, Brown University, Providence, RI, USA

[2] Center for Computation and Visualization, Brown University, Providence, RI, USA

[3] Research Improving People's Lives, Providence, RI, USA

[4] Division of Applied Mathematics, Brown University, Providence, RI, USA

[5] Department of Ecology and Evolutionary Biology, Yale University, New Haven, CT, USA

[6] Division of Infectious Diseases, The Alpert Medical School, Brown University, Providence, RI, USA

Abstract

Background: Phylogenetic analysis of HIV sequences obtained as part of clinical care is increasingly applied to detect clustering of new HIV infections and inform public health interventions to disrupt transmission. Conventional approaches summarize the within-host HIV diversity with a single consensus sequence per individual of only the *pol* gene, obtained from Sanger or next-generation sequencing (NGS).

Methods: We evaluate the robustness of the consensus approach and the potential benefits of considering the within-host diversity in phylogenetic analysis and cluster inference for all newly HIV-diagnosed individuals in the first half of 2013 at the largest HIV center in Rhode Island, USA. We compare Sanger and NGS-derived *pol* and near-whole genome consensus sequences to an alternate approach that samples many sequences per individual from a profile hidden Markov model of their NGS data.

Results: The space of phylogenies inferred through sampling is multi-modal, suggesting that a consensus-inferred phylogeny is not an appropriate summary of within-host variation. Cluster inference differs in phylogenies from consensus sequences from Sanger and NGS data, and across gene regions.

Discussion: The choice of sequencing and summarization methods affects the detection of clusters, and should be considered carefully in public health applications of phylogenetic analysis to disrupt HIV transmission.

Background

Clinicians are generally interested in inferring transmission links between HIV-infected individuals to inform and improve HIV treatment and prevention. In the absence of reliable patient contact histories, phylogenetic analysis of viral sequence data can be used to infer transmission clusters [1], under the assumption that two individuals sharing a most recent common ancestor in a phylogeny are more likely to share a transmission link in the real, unobservable transmission network. The application of phylogenetic analysis and cluster inference techniques in public health interventions to disrupt transmission was delineated as one of the four key pillars for achieving the Department of Health and Human Services' recently-announced plan for ending the HIV epidemic in the US [2].

While historically the phylogenetic informativeness of the *pol* region of the HIV genome was initially contested [3, 4], its use is now widespread in phylogenetic analysis and cluster inference, often due to the availability of *pol* sequences from routine clinical genotyping by commercial Sanger sequencing. In a meta study of published studies on HIV cluster inference, 98 out of 105 (93%) analyzed the *pol* region [5].

The increasing availability of NGS technology has led to longer and deeper sequencing of HIV, and data sets that cover nearly the whole genome with thousands or more reads at each site. Recent evidence suggests improvements in both phylogenetic analysis and cluster inference from near-whole genome HIV sequences obtained with NGS. For example, Yebra *et al.* [6] found that the accuracy of phylogenetic reconstruction and cluster inference on simulated sequences improved with longer genomic regions (with the best accuracy from a *gag*-*pol*-*env* concatenation). Novitsky *et al.* [7] similarly studied the effects on cluster inference of using longer genomic regions from real near-whole genome Sanger sequences, and found that the proportion of sequences in clusters increased with longer sequence regions.

While the advantages of longer sequences in inferring transmission have been demonstrated, the advantages of deeper sequencing have not yet been fully investigated. In part this is because researchers often rely on consensus sequences, since most phylogenetic methods require a single fully resolved sequence for each individual included in the phylogeny. Accordingly, researchers studying HIV transmission summarize the within-host HIV variation present in NGS data sets with a consensus sequence. In the larger context of phylogenetic methods (e.g. beyond their application to HIV sequences), this consensus approach carries an underlying statistical assumption of *low relative entropy* [8]. In the context of HIV, this assumption is that a consensus sequence can adequately capture all of the relevant information about within-host variation available in a deeply-sequenced NGS data set. Some previous studies of HIV transmission dynamics have accounted for this variation with coalescent within-host evolutionary models [9, 10], but such models still assume a consensus sequence as the observed data.

In this study, we examine how well this assumption underlying the consensus approach holds on an NGS data set comprising all newly HIV-diagnosed individual in the first six months of 2013 from the largest HIV center in Rhode Island, USA. We present a new approach called *profile sampling* that uses the within-host variation in the NGS data to assess the robustness of the consensus approach for phylogenetic analysis and cluster inference.

Methods

Data collection and sequencing

Our study and data collection were approved by Lifespan's Institutional Review Board. We collected viral sequences from 37 individuals newly diagnosed with HIV during 2013 and treated at The Miriam Hospital Immunology Center in Providence, Rhode Island, USA. Inclusion criteria were: (i) HIV-infected adults, 18 years of age or older; (ii) diagnosed with HIV during the first six months of 2013; and (iii) available *pol* sequence from routine drug resistance testing. Patient identifiers were removed and all analysis was conducted with de-identified sequence data.

We obtained near-whole genome viral sequences for the 37 participants using both Sanger and NGS sequencing methods. Blood specimens were obtained from participants with their consent and processed to isolate peripheral blood mononuclear cells (PMBC), buffy coats, and plasma. From the collected plasma, total nucleic acid was extracted for genotyping. An in-house genotyping assay was used to generate the near-whole genome based on previously published methods [11, 12]. For each sample, two cDNA templates were generated by SuperscriptIII First Strand Synthesis System (Thermofisher, Carlsbad, CA), followed by eight separate nested PCR reactions; these eight amplicons span the near-whole genome of HIV. Final amplicon products were sequenced by the Sanger method using 3100 Genetic Analyzer (Applied Biosystems, Foster City, CA) and sequenced by NGS using Nextera XT DNA Library Prep chemistry (Illumina, San Diego, CA) to generate multiplexed libraries for Illumina's MiSeq platform with 250 base paired-end reads. Sanger consensus sequences were generated manually using Sequencher version 5.2.4 (Gene Codes, Ann Arbor, MI) to confirm degenerate nucleotides. NGS data were processed and demultiplexed using BaseSpace cloud based application? (Illumina, San Diego, CA).

Profile sampling

We introduce a new approach for incorporating within-host variation into phylogentic analysis, called *profile sampling*. We start by aligning each individual's NGS reads using the hivmmer pipeline [13], which we extended to support near-whole genome HIV data and to perform codon-aware alignment within each gene (pending release as hivmmer version 0.3.0). A key feature of this pipeline is its use of profile hidden Markov models (HMMs) to model and align collections of HIV sequences. Profile HMMs have been used in many kinds of biological sequence analysis and are particularly well-suited to modeling variation in populations of sequences [14]. Briefly, hivmmer performs quality control and error correction in overlapping regions of the read pairs using PEAR version 0.9.11 [15], translates them into each possible reading frame, aligns them in amino acid space to profile HMMs of all group M reference sequences from the Los Alamos National Lab HIV Database with the profile HMM alignment tool HMMER version 3.1b2 [16], and produces a codon frequency table across the near-whole HIV genome. We refer to this resulting codon frequency table as the individual's HIV *profile*.

We construct fully-resolved sequences by sampling codons at each site in the genome using the codon frequencies from the profile. The collection of sampled sequences captures the empirical distribution of within-host variation at the codon level. We sample 500 sequences from each individual's profile, then collate the sampled sequences into 500 profile-sampled data sets, each having one sampled sequence per individual. We construct the 500 full-resolved sequences in order to use existing phylogenetic methods, because there is currently no published method to our knowledge for inferring a phylogeny directly from the proflie representation of the individual's within-host variation.

We perform phylogenetic inference on each of the 500 profile-sampled data sets by estimating a multiple sequence alignment with mafft version 7.313 [17] and a maximum-likelihood phylogeny with the GTRCAT model and 100 rapid bootstrap replicates using RAxML version 8.2.12 [18]. In addition to the 500 profile-sampled phylogenies, we infer two additional phylogenies from the NGS consensus sequences and Sanger consensus sequences with the same tools and parameters. We perform cluster inference on these phylogenies using Cluster Picker [19] with thresholds of 80% bootstrap support and 4.5% genetic distance. Analysis source code is available from `https://github.com/kantorlab/hiv-profile-sampling`.

In addition to performing these analyses on the near-whole genome sequences ("wgs"), we also perform them on subsets of the sequences in three clinicially relevant regions: the protease and reverse transcriptase regions at the beginning of the *pol* gene ("prrt"), the *int* gene, and the *env* gene. The prrt region and *int* are routinely sequenced in clinical care to detect drug resistance mutations and inform clinical choices of anti-retroviral therapy. The *env* region is... Rami, why is this routinely sequenced??

Results

Profile sampling estimates within-host diversity

We estimate the within-host diversity for individuals as the average percent difference across all pairwise comparisons of their 500 profile-sampled nucleotide sequences. These pairwise differences are calculated using the Hamming distance [20] (which is also called the *p*-distance in the literature on HIV genetic diversity [5, 21]). Figure 1 shows the estimated percent diversity in each region across individuals, ordered by *env*, which we expected *a priori* to be the most variable region. The largest estimated diversity is in *env* for individual MC28 (4.0%), and *env* has the largest range in estimated diversity (0.2% to 4.0%). The other regions have ranges of 0.2% to 1.9% (prrt), 0.1% to 2.0% (*int*) and 0.2% to 2.6% (wgs). These ranges are comparable to prior studies on within-host diversity [22, 23]. These estimates of within-host diversity from the HIV profiles suggest that the consensus approach is discarding potentially-relevant information that is present in the NGS data.

Phylogenetic estimates are sensitive to within-host diversity

Next, we investigate the impact of within-host diversity on phylogenetic topology and evolutionary distance estimates. To examine the variation in topology, we calculate the pairwise geodesic distance [24, 25] among the 500 phylogenies from the profile samples, as well as the phylogenies from the NGS and Sanger consensus sequences. Then we perform multi-dimensional scaling (MDS) on the resulting distance matrix to visualize the topological space in two dimensions (Figure 2). The results show that the topolical space is multi-model, and the consensus phylogenies inferred from the consensus sequences do not fully summarize the clustering that occurs in topological space. The prrt region displays four topological clusters, and the NGS and Sanger consensus phylogenies are located in difference clusters. There are two clusters in *int*, and the NGS consensus phylogeny lies at the center of one of the clusters, while the Sanger consensus phylogeny is an outlier. The consensus phlyogenies lie at opposite ends of the primary MDS axis in *env*, and of the secondary MDS axis in the wgs region.

To examine the variation in estimated evolutionary distance, we sum the branch lengths within each phylogeny across all branches and across only the tip branches. We visualize the distribution of these branch length sums in Figure 3. Overall, the estimates are larger in *env* and the wgs region, and smaller when restricting to only the tip branches. In some cases, the consensus phylogenies provide an adequate summary of the distribution (as in Sanger consensus phylogeny for all branches in *env*, or the NGS consensus phylogeny for tip branches in *env*). In other cases, the consensus phylogenies have estimates that are outliers in the distribution (as in both consensus phylogenies for either all or tip branches in the prrt region).

Taken together, these results demonstrate that within-host diversity is associated with variation in phylogenetic estimates, and that the consensus approach provides only a point estimate that does not always adeuqatley summarize the underlying variation. For example, the variation can be multi-modal and the point estimates from the consensus phylogenies can be outliers.

Inferred clusters differ by sequencing method and genomic region

Finally, we examine the clusters that are detected in the NGS versus Sanger consensus phylogenies, and across the four regions. The NGS consensus phylogeny detects 8 clusters in prrt, 9 in *int*, 4 in *env*, and 6 in wgs. Each cluster appears as a colored bar in the phylograms in Figure 4. We use the proportion of times a cluster appears across the 500 profile-sampled phylogenies as a measure of support for that cluster, and report it next to the colored bar. Some clusters are robustly detected across all regions, such as the cluster (MC25, MC26, MC52), which has support between 98% and 100%. Other clusters are detected at lower support, and are not detected consistently across regions. For example, cluster (MC14, MC59) only appears in the *int* and wgs phylogenies, and at 60% to 62% support.

The Sanger consensus phylogeny detects 8 clusters in prrt, 7 in *int*, 6 in *env*, and 7 in wgs (Figure 5). As with the NGS consensus phylogeny, the support and consistency of cluster detection varies across regions. Cluster detection is mostly consistent with the NGS consensus, except for the cluster (MC17, MC21), which only occurs in *env* in the Sanger consensus, and has zero support from the profile samples. Three clusters are consistently detected across NGS and Sanger, and across all regions: (MC23, MC24); (MC25, MC26, MC52); and (MC27, MC28).

Discussion

Our study provides new evidence on the utility of NGS HIV sequencing for phylogenetic analysis and cluster inference. The deeper sequencing provided by NGS can measure within-host diversity that is associated with variation in phylogenetic estimates. This variation is in turn associated with differences in cluster detection, which could have epidemiological consequences as public health officials increasingly look to cluster inference as a tool for informing and improving HIV prevention and treatment. Current approaches to HIV cluster inference almost exclusively use Sanger *pol* consensus sequences, due to their availability from routine genotyping. In our results, this approach uncovers 8 clusters; however, only 3 of the 8 are robustly detected across regions and in both NGS and Sanger consensus sequences.

In our comparison of cluster inference across genomic regions, we found that fewer clusters were detected overall in *env* and wgs compared to prrt and *int*. Prior studies of clustering from Sanger consensus sequences present mixed results on the prevalence of clustering across regions. Some studies have found concordant clustering across *gag*-*env* [26] and *gag*-*pol*-*env* [27, 28], while others found fewer clusters in *pol* than in *env* [29], or fewer clusters in *gag*-*env* than in *pol* [30]. The additional information available in NGS data, along with the cluster support measures provided by profile sampling, may help resolve these differences. In our results, for example, the cluster support measure establishes four clusters with robust support ($\geq$95%) in only prrt and *int*: (MC37, MC53); (MC17, MC20, MC21); (MC41, MC47, MC56); and (MC45, MC58).

A limitation of our study is the small number of participants. The participants have a dense temporal sampling, and comprise all newly HIV-diagnosed individuals in a six month period at the largest HIV center in Rhode Island, USA, who met the inclusion criteria. The overall size of the HIV epidemic in Rhode Island is much larger, estimated as 2,396 individuals in 2016 [31], but NGS data for this population are not currently available beyond those presented in this study. In future work, however, we hope to apply the profile sampling method to larger NGS data sets, to assess if cluster inference from Sanger versus NGS data agrees or differs especially for clusters larger than three individuals, which was the largest cluster size in this study.

Our construction of HIV profiles from NGS data is limited by the accuracy of the NGS assays themselves. The codon frequencies in the profiles may be biased measures of the true within-host diversity because of biases in PCR amplification during sample preparation. Sequencing protocols such as Primer ID [32] have been introduced to reduce and correct for these biases. Unfortunately, the Primer ID protocol supports only a limited region of the HIV genome, and has not yet been extended to support near-whole genome sequencing of HIV, but future work could study this limited region to determine if cluster inference changes with the implementation of a Primer ID protocol.

The true HIV transmission network is unknown, but phylogenetic analysis and cluster inference are promising tools for aiding clinicians and public health officials [2]. Current phylogenetic approaches do not fully utilize the information on within-host diversity available in near-whole genome NGS data. As NGS data sets are increasingly available and become more representative of the current HIV epidemic, the additional information they measure has the potential to improve the robustness of cluster inference.

Acknowledgments

Mia Coetzer, Lauren Ledingham, Matt D'Antuono, Philip A. Chan

References

1. Leitner, T, Escanilla, D, Franzen, C, Uhlen, M, and Albert, J. Accurate reconstruction of a known HIV-1 transmission history by phylogenetic tree analysis. Proceedings of the National Academy of Sciences 1996;93:10864–10869.
2. Fauci, AS, Redfield, RR, Sigounas, G, Weahkee, MD, and Giroir, BP. Ending the HIV Epidemic: A Plan for the United States. JAMA 2019;321:844.
3. Hué, S, Clewley, JP, Cane, PA, and Pillay, D. HIV-1 pol gene variation is sufficient for reconstruction of transmissions in the era of antiretroviral therapy. AIDS 2004;18:719–728.
4. Stürmer, M, Preiser, W, Gute, P, Nisius, G, and Doerr, HW. Phylogenetic analysis of HIV-1 transmission: pol gene sequences are insufficient to clarify true relationships between patient isolates. AIDS 2004;18:2109–2113.
5. Hassan, AS, Pybus, OG, Sanders, EJ, Albert, J, and Esbjörnsson, J. Defining HIV-1 transmission clusters based on sequence data: AIDS 2017;31:1211–1222.
6. Yebra, G, Hodcroft, EB, Ragonnet-Cronin, ML, et al. Using nearly full-genome HIV sequence data improves phylogeny reconstruction in a simulated epidemic. Scientific Reports 2016;6:39489.
7. Novitsky, V, Moyo, S, Lei, Q, DeGruttola, V, and Essex, M. Importance of Viral Sequence Length and Number of Variable and Informative Sites in Analysis of HIV Clustering. AIDS Research and Human Retroviruses 2015;31:531–542.
8. Guang, A, Zapata, F, Howison, M, Lawrence, CE, and Dunn, CW. An Integrated Perspective on Phylogenetic Workflows. Trends in Ecology & Evolution 2016;31:116–126.
9. Giardina, F, Romero-Severson, EO, Albert, J, Britton, T, and Leitner, T. Inference of Transmission Network Structure from HIV Phylogenetic Trees. PLOS Computational Biology 2017;13:e1005316.
10. Romero-Severson, E, Skar, H, Bulla, I, Albert, J, and Leitner, T. Timing and Order of Transmission Events Is Not Directly Reflected in a Pathogen Phylogeny. Molecular Biology and Evolution 2014;31:2472–2482.
11. Nadai, Y, Eyzaguirre, LM, Constantine, NT, et al. Protocol for Nearly Full-Length Sequencing of HIV-1 RNA from Plasma. PLoS ONE 2008;3:e1420.

12. Di Giallonardo, FD, Töpfer, A, Rey, M, et al. Full-length haplotype reconstruction to infer the structure of heterogeneous virus populations. Nucleic Acids Research 2014;42:e115–e115.

13. Howison, M, Coetzer, M, and Kantor, R. Measurement error and variant-calling in deep Illumina sequencing of HIV. Bioinformatics 2019;35:2029–2035.

14. Eddy, SR. What is a hidden Markov model? Nature Biotechnology 2004;22:1315–1316.

15. Zhang, J, Kobert, K, Flouri, T, and Stamatakis, A. PEAR: a fast and accurate Illumina Paired-End reAd mergeR. Bioinformatics 2014;30:614–620.

16. Eddy, SR. Accelerated Profile HMM Searches. PLOS Computational Biology 2011;7:e1002195.

17. Katoh, K and Standley, DM. MAFFT Multiple Sequence Alignment Software Version 7: Improvements in Performance and Usability. Molecular Biology and Evolution 2013;30:772–780.

18. Stamatakis, A. RAxML Version 8: A tool for Phylogenetic Analysis and Post-Analysis of Large Phylogenies. Bioinformatics 2014:btu033.

19. Ragonnet-Cronin, M, Hodcroft, E, Hué, S, et al. Automated analysis of phylogenetic clusters. BMC Bioinformatics 2013;14:317.

20. Allam, O, Samarani, S, and Ahmad, A. Hammering out HIV-1 incidence with Hamming distance: AIDS 2011;25:2047–2048.

21. Maldarelli, F, Kearney, M, Palmer, S, et al. HIV Populations Are Large and Accumulate High Genetic Diversity in a Nonlinear Fashion. Journal of Virology 2013;87:10313–10323.

22. Li, G, Piampongsant, S, Faria, NR, et al. An integrated map of HIV genome-wide variation from a population perspective. Retrovirology 2015;12:18.

23. Zanini, F, Brodin, J, Thebo, L, et al. Population genomics of intrapatient HIV-1 evolution. eLife 2015;4:e11282.

24. Billera, LJ, Holmes, SP, and Vogtmann, K. Geometry of the Space of Phylogenetic Trees. Advances in Applied Mathematics 2001;27:733–767.

25. Owen, M and Provan, JS. A Fast Algorithm for Computing Geodesic Distances in Tree Space. IEEE/ACM Transactions on Computational Biology and Bioinformatics 2011;8:2–13.

26. Han, Z, Leung, TW, Zhao, J, et al. A HIV-1 heterosexual transmission chain in Guangzhou, China: a molecular epidemiological study. Virology Journal 2009;6:148.

27. English, S, Katzourakis, A, Bonsall, D, et al. Phylogenetic analysis consistent with a clinical history of sexual transmission of HIV-1 from a single donor reveals transmission of highly distinct variants. Retrovirology 2011;8:54.

28. Kaye, M, Chibo, D, and Birch, C. Phylogenetic Investigation of Transmission Pathways of Drug-Resistant HIV-1 Utilizing Pol Sequences Derived From Resistance Genotyping: JAIDS Journal of Acquired Immune Deficiency Syndromes 2008;49:9–16.

29. Kapaata, A, Lyagoba, F, Ssemwanga, D, et al. HIV-1 Subtype Distribution Trends and Evidence of Transmission Clusters Among Incident Cases in a Rural Clinical Cohort in Southwest Uganda, 2004–2010. AIDS Research and Human Retroviruses 2013;29:520–527.

30. Ndiaye, HD, Tchiakpe, E, Vidal, N, et al. HIV Type 1 Subtype C Remains the Predominant Subtype in Men Having Sex with Men in Senegal. AIDS Research and Human Retroviruses 2013;29:1265–1272.

31. Rhode Island Department of Health. HIV Progress [Internet]. Available from: https://health.ri.gov/data/hiv/. [Accessed 12 Dec 2019]. 2019.

32. Jabara, CB, Jones, CD, Roach, J, Anderson, JA, and Swanstrom, R. Accurate sampling and deep sequencing of the HIV-1 protease gene using a Primer ID. Proceedings of the National Academy of Sciences 2011;108:20166–20171.

Figure 1: Intra-patient genetic diversity (defined as the average percent difference across all pairwise comparisons of the 500 profile-sampled nucleotide sequences for a patient) is highest in *env* for most individuals, and lies within the range of previously reported values.

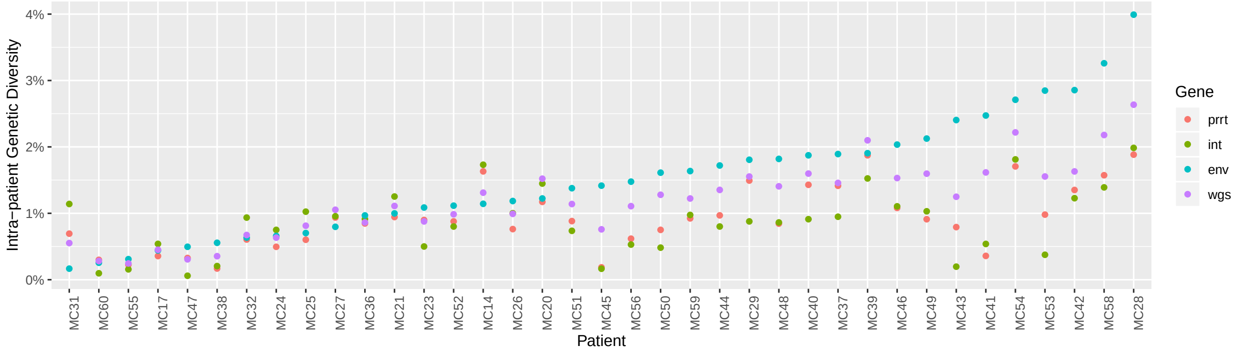

Figure 2: Multi-dimensional scaling of pairwise geodesic distance among maximum-likelihood phylogenies from the profile-sampling approach show that the space of phylogenies inferred for the prrt and int regions are multi-modal. The phylogenies from consensus sequences (black dots) are point estimates that do not capture the full variation in phylogenies that can be inferred from deeply-sequenced NGS data.

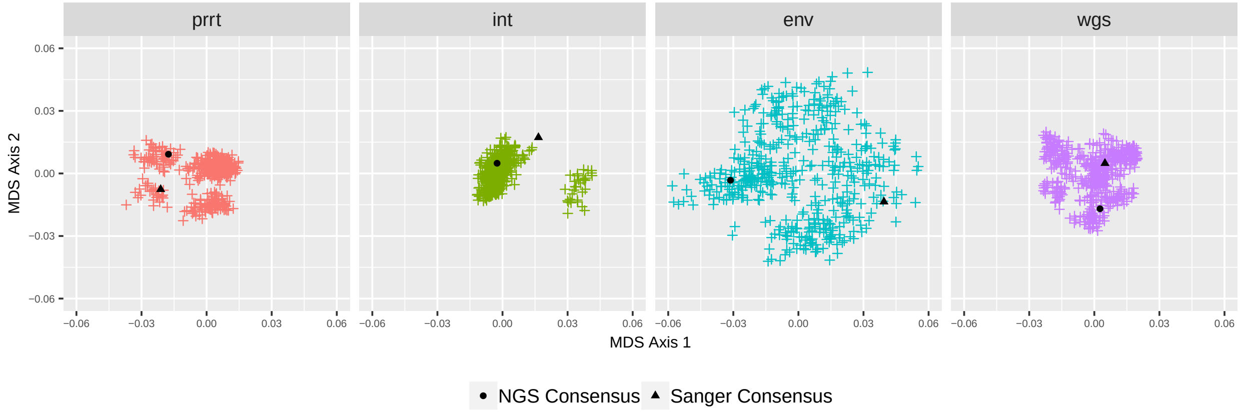

Figure 3: The total branch length in each of the profile-sampled phylogenies also varies. The phylogenies from consensus sequences (black dots) can lie at extreme values within these distribution, both when considering the lengths across all branches and the lengths across only the branches at the tips.

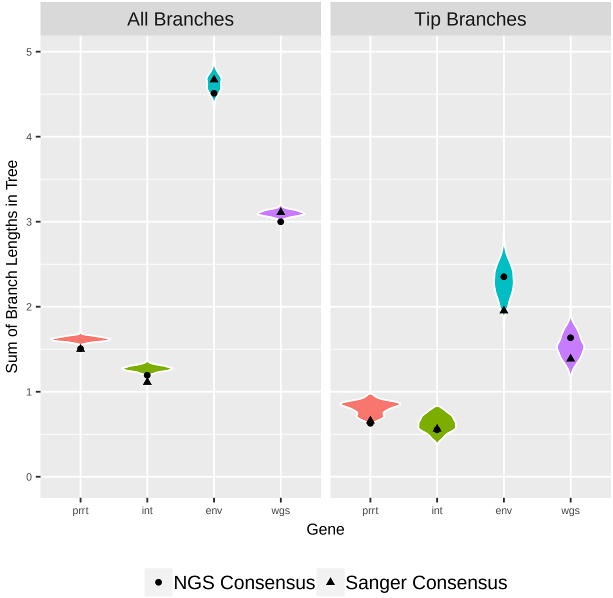

Figure 4: Clusters (vertical colored bars) inferred from the phylogenies of NGS consensus sequences differ across genomic regions. The largest number of clusters was inferred from the int region, and the smallest number from the env region. Profile sampling provides a bootstrapped measure of cluster support (annotation to bars).

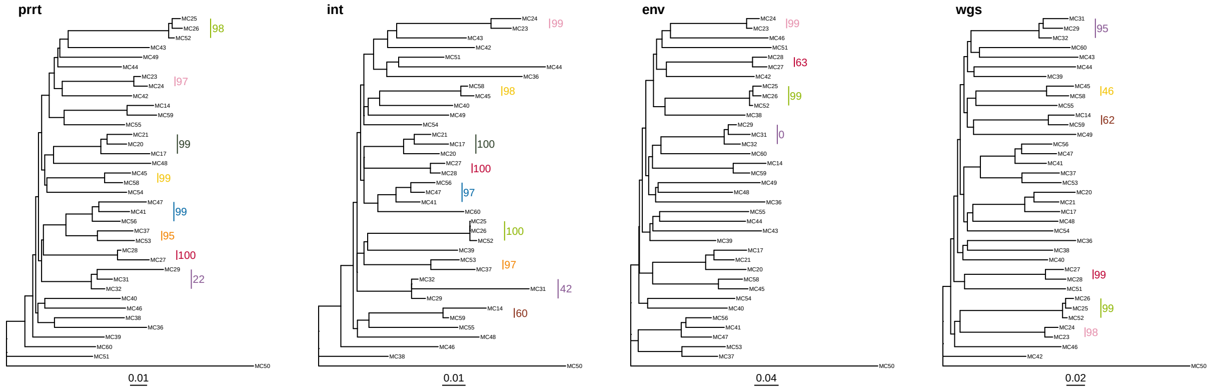

Figure 5: Clusters (vertical colored bars) inferred from the phylogenies of Sanger consensus sequences differ across genomic regions. The largest number of clusters was inferred from the int region, and the smallest number from the env region. Profile sampling provides a bootstrapped measure of cluster support (annotation to bars).

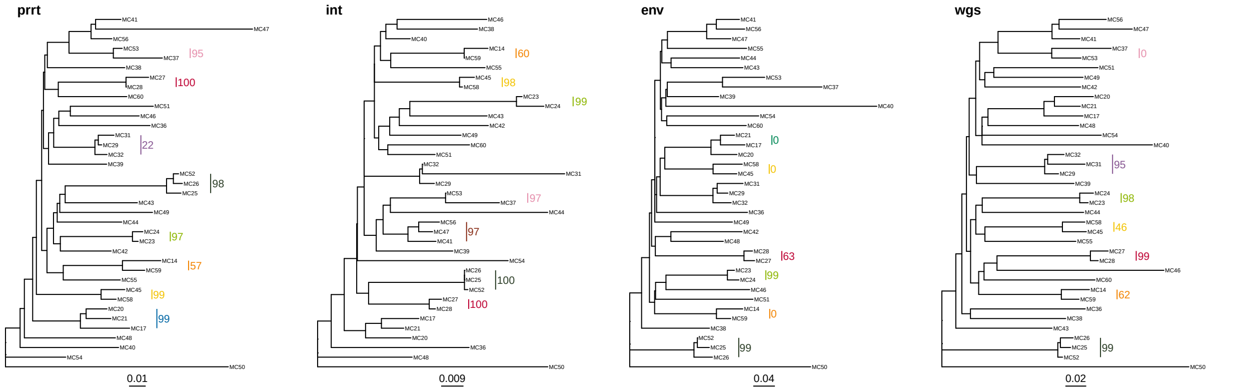

Figure 6: Summary of clusters identified by Sanger versus NGS consensus sequences across genomic regions. Numeric values indicate bootstrapped cluster support from the profile sampling method. A blank cell indicates that the cluster was not detected in that consensus sequence and genomic region.

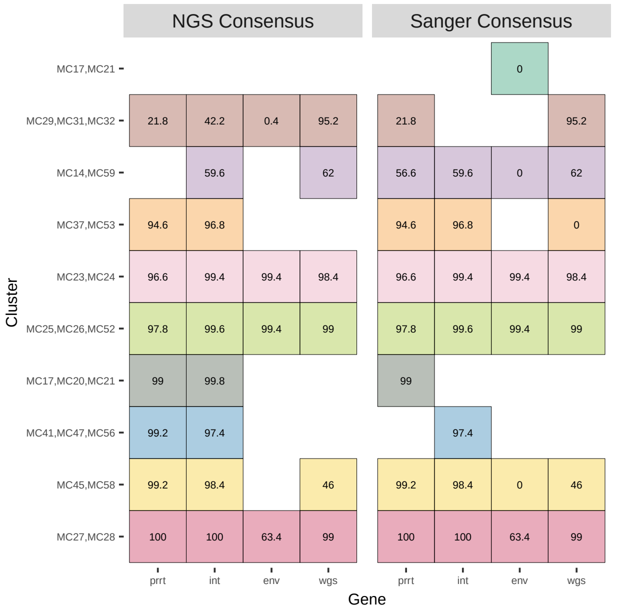
NGS Consensus
Sanger Consensus
MC17,MC21
MC29,MC31,MC32
MC14,MC59
MC37,MC53
MC23,MC24
MC25,MC26,MC52
MC17,MC20,MC21
MC41,MC47,MC56
MC45,MC58
MC27,MC28
Cluster
prrt
int
env
wgs
prrt
int
env
wgs
Gene